Application of Near-Infrared Spectroscopy to Determine the Juvenile–Mature Wood Transition in Black Spruce

Guillaume Giroud
Maurice Defo
Jean Bégin
Chhun-Huor Ung

Abstract

The potential of near-infrared spectroscopy (NIRS) to determine the transition from juvenile to mature wood in black spruce (*Picea mariana* (Mill.) B.S.P.) was assessed. In total, 127 wood samples were harvested from 50 sites located across the black spruce–moss domain in the province of Québec, Canada. Mechanical wood properties were determined by SilviScan. NIR spectra were collected on the transverse face of the samples. Good to excellent calibration statistics (R^2, ratio of performance to deviation) were obtained for basic density (0.85, 1.8), microfibril angle (0.79, 2.2), and modulus of elasticity (0.88, 2.9). Two-segment linear regressions were applied to microfibril angle profiles to determine the transition age and then calculate the juvenile and mature wood properties. The values obtained using SilviScan data were compared with those obtained using NIRS predicted data. Using SilviScan data, the average transition age was 23 years, with a standard deviation of 7 years. The correlation was moderate for the transition age ($r = 0.592$, $P < 0.0001$), which was slightly underestimated by NIRS with a mean prediction error (and 95% limits of agreement) of -2.2 ± 6.3 years ($-14.6/10.1$). These results suggest that the transition age from juvenile to mature wood could be predicted by NIRS. This article makes some recommendations to improve method accuracy for operational use.

Natural variation in black spruce (*Picea mariana* (Mill.) B.S.P.) wood properties is known, which is not the case for its spatial variation. There is presently no spatial information produced by the provincial forest inventory programs of Canada on fiber quality. This lack of knowledge is problematic for plant supplies. This knowledge could be integrated into decision support systems in order to improve and optimize forest management and the entire value chain (Briggs 2010). Black spruce is one of the main commercial species in the Canadian boreal forest (Viereck and Johnston 1990). Its principal commercial use is for high-quality pulp manufacturing. It is also largely used for lumber and high-value building products. Black spruce grows on a wide variety of sites, suggesting a potential spatial variation in wood properties. Lessard et al. (2014) recently demonstrated that it was possible to model and map wood properties at the landscape level for black spruce and balsam fir (*Abies balsamea*) in Newfoundland. In Québec, the provincial government is also planning to model and map wood properties of the main commercial species of the boreal forest by 2020. To this end, the present study aims to evaluate the potential of near-infrared spectroscopy (NIRS) to quickly and accurately characterize the fiber properties of wood samples.

NIRS is used in many industrial applications because of its numerous advantages. It is cost and time effective, relatively accurate, and nondestructive. The use of NIRS by

The authors are, respectively, PhD Scholar, Researcher, and Professor, Dépt. des Sci. du bois et de la forêt, Faculté de foresterie, de géographie et de géomatique, Univ. Laval, Québec, Canada (Guillaume.Giroud@mffp.gouv.qc.ca [corresponding author], Maurice.Defo@sbf.ulaval.ca, Jean.Begin@sbf.ulaval.ca); and Retired Researcher, Natural Resources Canada, Canadian Forest Serv., Canadian Wood Fibre Centre, Québec, Canada (chhunhuorung@gmail.com). This paper was received for publication in April 2014. Article no. 14-00045.

Forest Prod. J. 65(3/4):129–138.
doi:10.13073/FPJ-D-14-00045

the forest and forest products industries has been increasing over the past 20 years (Tsuchikawa 2007, Meder et al. 2010). During the last decade, a lot of efficient NIRS calibration models were built using SilviScan data (for example, see Schimleck et al. 2001, Jones et al. 2005). Today, NIRS seems to be the most economic method when dealing with thousands of wood samples. NIR light interacts with material, and the spectral response can be interpreted using multivariate analysis (Siesler et al. 2002). NIRS does not directly measure anatomical or physical properties of wood. It measures the absorption of NIR light by the sample. This absorption occurs when the NIR frequency is the same as the vibrational frequency of a molecular bond. The NIR signal is thus sensitive to changes in wood chemistry. Furthermore, the wood chemistry varies with age. For instance, the microfibril orientation in the S2 layer appears related to lignin content in normal wood with a decrease of microfibril angle (MFA) and lignin content from pith to bark (Via et al. 2009, Hein et al. 2010). These findings help give us a better understanding of how MFA can be predicted by NIRS. Xu et al. (2011) have successfully used NIRS data to predict wood density and modulus of elasticity based on SilviScan measurements for black spruce and balsam fir. However, they found that MFA was not well estimated by NIRS, unlike the results obtained with other species (Schimleck and Evans 2002, Jones et al. 2005, So et al. 2013). The potential of NIRS to predict the wood properties of increment cores has largely been demonstrated. Nevertheless, to our knowledge, the potential of NIRS to model MFA in order to automatically determine the transition from juvenile to mature wood has never been studied.

The first growth rings from the pith form the juvenile wood (Panshin and De Zeeuw 1980, Jozsa and Middleton 1994). Its formation is controlled by the action of phytohormones and the aging process. The transition from juvenile to mature wood occurs at a given time called *transition age*. The mechanical properties of mature wood are stronger and present very few variations, unlike those of juvenile wood. Juvenile wood is undesirable for many applications. The industry tries to reduce its content by tree breeding and silvicultural treatments. There is no universally accepted definition of the transition age from juvenile to mature wood. It can be determined using different wood properties and different mathematical methods such as the threshold method, polynomial regression, segmented regression, or derivative function. These methods were assessed on different ring properties such as density, surface area, percentage of latewood, MFA, and tracheid length (Yang and Hazenberg 1994, Alteyrac et al. 2006, Clark et al. 2006). As shown by Alteyrac et al. (2006), the transition age varies according to wood property considered and the method used. In our study, MFA and linear segmented regression were used. The two-segment linear regression (TSLR) is one of the most widely used methods to determine the transition point. TSLR has often been applied on MFA profiles (Bhat et al. 2001, Alteyrac et al. 2006, Clark et al. 2006, Wang and Stewart 2012). Wang and Stewart (2012) assessed different forms of two-segmented regression (linear, quadratic, exponential, and constant) to estimate MFA transition point, but concluded that all combinations give essentially the same estimates from a practical viewpoint.

The MFA profile generally follows the same pattern from the pith to the bark (Donaldson 2008). It decreases rapidly in the juvenile wood portion and remains more or less stable in the mature wood portion, unless compression wood is present. The MFA profile thus presents an inverted J-shaped pattern. However, the rate of decrease in MFA with age varied among species. In hardwoods, similar patterns occur, but with much less variation and much smaller MFAs in juvenile wood. MFA is influenced by environmental factors as shown by its increased values in compression wood, decreased values in tension wood, and often increased values following nutrient or water supplementation. This typical inverted J shape was observed for MFA in black spruce (Alteyrac et al. 2006). Similar profiles were also observed for pine species (Schimleck and Evans 2002, Wang and Stewart 2012), eucalyptus (Evans et al. 2000), and teak (Bhat et al. 2001). MFA profiles show two interesting features in softwoods: a typical behavior in the presence of compression wood and a high variability from the pith to the bark. MFA usually decreases from the pith to the bark. In a sample with no defect, any sudden increase in MFA can be attributed to compression wood (Barnett and Bonham 2004). Compression wood is formed under stress conditions. The presence of compression wood disturbs the MFA profile and makes it difficult to determine the transition point. However, it is easy to detect and remove the disruptions caused by the presence of compression wood in order to recover the normal pattern. Finally, MFA decreases greatly from the pith to the bark. The values are around three times lower in black spruce mature wood than in juvenile wood (Alteyrac et al. 2006). This characteristic should thus facilitate determination of the transition point by TSLR.

The aim of this study was to develop a quantitative, economic, and accurate method to determine the transition age from juvenile to mature wood in black spruce. The working hypothesis is that the transition age from juvenile to mature wood can be estimated by applying the TSLR method to MFA profiles predicted by NIRS. Once the transition age is known, it becomes possible to calculate the average properties for each wood type. This method could be easily integrated into a NIRS system to produce real-time estimates of transition age and juvenile–mature wood properties for an increment core. In this study, basic density (BD), MFA, and modulus of elasticity (MOE) were investigated in relation to juvenile and mature wood.

Materials and Methods

Sample origin and preparation

In the 2000s, the Québec provincial government implemented a large-scale forest inventory program to develop site index and taper equations for the main commercial species. In total, 1,648 plots were sampled in the main ecological regions. About 14,000 trees were harvested and cut into disks for ring analysis. At the end of the program, thousands of disks were selected and kept frozen by the federal government for future research. For this study, 127 wood disks cut at breast height were selected. They were from 50 sites located in the black spruce–moss domain. The sites were chosen to take into account the ecological variability of the study area. The trees were between 45 and 148 years old. The 127 samples were cut in radial sticks of 17 by 10 mm (tangentially by longitudinally). NIRS

measurement is sensitive to wood moisture content (Xu et al. 2011), surface preparation (Schimleck et al. 2005a), and cell orientation (Schimleck et al. 2005b). Therefore, more attention was paid to these parameters. Wood surface was sanded using three sandpaper grits (120, 220, and 320) and then cleaned up to remove dust. The radial sticks were conditioned for several days at 60 percent relative humidity and 20°C to reach a wood moisture content of 12 percent.

Near-infrared spectroscopy

Fourier Transform (FT) NIR spectra were acquired with a Perkin Elmer Spectrum 400 FT-MIR/FT-NIR spectrometer, using near-infrared reflectance accessory (NIRA). The diameter of the NIRA opening was 15 mm. Black electrical masking tape, which fully absorbs NIR light, was used to reduce the opening to 5 by 5 mm in order to be closer to the size of increment cores as usually collected in eastern Canada. Only the transverse face of cores is usually prepared and sanded for ring analysis. Hence the NIRS calibrations were developed with the transverse face even though SilviScan works with the radial face. Furthermore Schimleck et al. (2005b) tested NIRS calibrations on both faces of SilviScan samples for air-dry density, MFA, MOE, and several tracheid morphological characteristics. They concluded that the differences between the two sets were small, indicating that either face could be used for NIR analysis. The spectra were collected from the bark side to the pith in 7.5-mm increments. These spectra were initially collected for other reasons. For the purposes of this study, a 5-mm increment size would have been more justified, but the samples were already cut in sticks according to SilviScan's specifications. The spectra were collected over the wavelength range of 680 to 2520 nm, at 1-nm intervals. Thirty-two scans were accumulated and averaged to give a single spectrum by spot. A ceramic standard was used as instrument reference. In total, 1,332 spectra were collected from the 127 samples.

SilviScan analysis

The same 127 radial sticks were then analyzed by SilviScan-3 at FPInnovations in Vancouver, British Columbia. SilviScan processing was precisely described by Cieszewski et al. (2013). The samples were cut into radial strips of 2 by 7 mm (tangentially by longitudinally) and conditioned at 40 percent relative humidity and 20°C to reach a wood moisture content of 8 percent (dry basis). No acetone extraction was performed because the NIR models are intended to be used on increment cores with no extraction. Wood density was determined at a 25-μm radial resolution using the X-ray densitometer unit of SilviScan. MFA was determined at a 5-mm radial resolution using the X-ray diffractometer unit. MOE was estimated using the density and the coefficient of variation of the X-ray diffraction profile intensity (Evans 1999). The density at 8 percent moisture content was converted into basic density as follows (Siau 1995):

$$\mathrm{BD} = \frac{1{,}000 \times D_8}{1{,}080 + 0.22 \times D_8}$$

where BD is basic density and D_8 is density at 8 percent moisture content. It is assumed that the fiber saturation point is 30 percent and that the water density is 1,000 kg/m^3.

Development of NIR calibrations

SilviScan values were matched with the corresponding NIR spots according to measurement position. Data processing was used to prepare and match the databases (PROC SQL, SAS 9.3). For statistical purposes, 34 sites were randomly chosen for the calibration set (88 samples, 918 spectra) and 16 others for the validation set (39 samples, 414 spectra). Multivariate data analysis was performed using The Unscrambler X software (version 10.2, Camo, Oslo, Norway). The presence of outliers was evaluated using the Hotelling T^2 ellipse on principal components analysis (PCA) scores plots with a 99 percent confidence interval. Model calibration and validation were performed using partial least-squares (PLS) regression. Calibration models were developed with four random cross-validation segments. Several combinations of wavelength ranges and mathematical pretreatments (smoothing, baseline offset, Savitzky-Golay derivatives, and multiplicative scatter correction) were tested. The optimal number of principal components was suggested by the software, based on the significance of the change in explained variance. In addition, to test the model on a validation set, a full cross-validation procedure was also applied on the calibration set. The calibration performance was assessed using the coefficient of determination (R^2c), the standard error of calibration (SEC), the standard error of cross-validation (SECV), and the ratio of performance to deviation (RPDc) calculated as the ratio of standard deviation of the reference data to SECV (Williams and Sobering 1993, Jones et al. 2005). The calibration model was then tested on the validation set. The standard error of prediction (SEP) gave a measure of how well the calibration predicted the wood property of the remaining 414 spots (validation set). The predictive ability of the calibration was also assessed using the ratio of performance to deviation (RPDv).

Segmented regression analysis

TSLRs were applied to MFA profiles to determine the transition age from juvenile to mature wood for the 127 samples. Models were built with MFA values measured by SilviScan and MFA values predicted by NIRS. The transition age is frequently expressed in terms of number of rings from the pith (Wang and Stewart 2012). Each ring MFA value was determined from the 5-mm increment MFA profile using data processing (PROC SQL, SAS 9.3). A mathematical pretreatment was applied on MFA profiles to remove the effect of compression wood. Any sudden MFA increase above 0.025° per mm was removed. This threshold was chosen by trial and error.

A TSLR model can be written as follows (Ryan and Porth 2007):

$$y_i = a_1 + b_1 x_i + \varepsilon \quad \text{for} \, x \leq c$$

and

$$y_i = a_2 + b_2 x_i + \varepsilon \quad \text{for} \, x > c$$

where y_i is the MFA value of the ith ring from the pith, x_i is the ith ring, a_1 is the intercept of linear fit to data below the estimated breakpoint, b_1 is the slope of linear fit to data below the estimated breakpoint, a_2 is the intercept of linear fit to data above the estimated breakpoint, b_2 is the slope of linear fit to data above the estimated breakpoint, c is the estimated breakpoint, and ε is the error term. The transition

Table 1.—Statistics of wood properties for the near-infrared calibration and validation sets.[a]

	Calibration set				Validation set			
Wood property	*n*	Mean (SD)	Min.	Max.	*n*	Mean (SD)	Min.	Max.
BD (kg/m^3)	918	428.3 (42.8)	324.2	609.4	414	425.8 (47.4)	293.6	632.8
MFA (degrees)	918	16.9 (7.0)	8.0	47.4	414	18.1 (8.0)	8.1	52.1
MOE (GPa)	918	12.4 (3.7)	4.1	21.9	414	12.0 (3.9)	4.7	21.8

[a] BD = basic density; MFA = microfibril angle; MOE = modulus of elasticity.

point (c) is the intersection point of two lines, which is obtained as follows:

$$c = \frac{a_2 - a_1}{b_1 - b_2}$$

The first step in applying a segmented regression is to graph the data to estimate visually where the break occurs (Ryan and Porth 2007). The transition age seemed to vary between 10 and 40 years for the 127 MFA profiles obtained from SilviScan. An automatic procedure was developed (1) to estimate all the possible starting parameters (a_1, b_1, b_2, c) for transitions between 10 and 40 years using regression analysis (PROC REG, PROC NLIN, SAS 9.3) and (2) to choose the model with the smallest mean squared error using data processing (PROC SQL, SAS 9.3). Once the transition point was determined, the proportions of juvenile and mature wood were calculated, as well as the average values of BD, MOE, and MFA. These juvenile and mature wood properties were obtained by calculating the area-weighted mean, assuming a circular shape of the rings.

Methods comparison for the determination of wood properties

The ability of a model to precisely predict the value from a single sample can be assessed using statistics such as RPD for NIRS models. However, the analysis of population statistics is also a good way to assess the calibration performance. Average wood properties and transition ages determined using SilviScan data were thus compared with values obtained using NIRS predicted data. The comparison was assessed using the Pearson correlation coefficient (r), the mean prediction error (bias), and the 95 percent limits of agreement. High correlation means that data from the two methods are linearly related, even if they cannot agree. The mean prediction error is the mean difference between the measurements of the two methods (Bland and Altman 1995). The closer the mean prediction error is to zero, the less bias there is. The lower and upper limits represent the 95 percent limits of agreement of the mean difference ($\pm 1.96 \times$ SD). The smaller the range between these two limits, the better the agreement.

Results and Discussion

SilviScan wood properties

The statistics of wood properties were calculated using SilviScan data of the 127 samples. Average values were 431.8 $\pm$ 31.2 kg/m^3 in BD, 14.1 $\pm$ 2.3 GPa in MOE, and 14.0° $\pm$ 3.1° in MFA. The average BD value was similar to that measured by Jessome (1995). Lessard (2013) obtained similar MOE and MFA values for black spruce samples from 77 sites across Newfoundland, with average values of 13.9 $\pm$ 2.3 GPa in MOE and 15.6° $\pm$ 3.3° in MFA. The statistics of wood properties were also calculated for the calibration set (88 samples, 918 spectra) and for the independent validation set (39 samples, 414 spectra) for the purpose of comparison (Table 1). Average values for the calibration set were slightly lower for MFA (16.9° vs. 18.1°) but very similar to those of the validation set for BD (428.3 vs. 425.8 kg/m^3) and MOE (12.4 vs. 12.0 GPa).

Development of NIR calibrations

Table 2 presents the calibration statistics obtained for BD, MOE, and MFA by PLS regression. No outlier was observed or removed. None of mathematical pretreatments significantly improved the precision of the models. Calibration statistics (R^2c, SECV) were higher for MOE (0.89, 1.3) than for BD (0.82, 25.0) or MFA (0.82, 3.1). The wavelength range and the number of principal components (PC) were also smaller for MOE (900 to 1,150 nm, 6 PC) than for BD (900 to 2,500 nm, 8 PC) or MFA (680 to 2,500 nm, 9 PC). The models were then tested on the validation set (39 samples, 16 sites, 414 spectra; Table 2). The statistics (R^2v, SEP, RPDv) did not drop off when predicting BD (0.85, 26.0, 1.8), MFA (0.79, 3.6, 2.2), or MOE (0.88, 1.3, 2.9). SEC and SEP values were very similar for all wood properties.

Good to excellent calibrations were thus obtained for BD, MOE, and MFA. In other words, in this study, strong linear

Table 2.—Summary of near-infrared calibration and validation statistics.[a]

	Calibration set							Validation set			
Wood property	*n*	Range	PC	R^2c	SEC	SECV	RPDc	*n*	R^2v	SEP	RPDv
BD (kg/m^3)	918	900–2,500	8	0.82	24.2	25.0	1.71	414	0.85	26.0	1.82
MFA (degrees)	918	680–2,500	9	0.82	3.0	3.1	2.29	414	0.79	3.6	2.22
MOE (GPa)	918	900–1,150	6	0.89	1.2	1.3	2.91	414	0.88	1.3	2.93

[a] PC = number of principal components; R^2c = coefficient of determination for calibration set; SEC = standard error of calibration; SECV = standard error of cross-validation for calibration set; RPDc = ratio of performance to standard deviation for calibration set; R^2v = coefficient of determination for validation set; SEP = standard error of prediction; RPDv = ratio of performance to standard deviation for validation set; BD = basic density; MFA = microfibril ange; MOE = modulus of elasticity.

relationships were obtained between the studied wood properties and the absorption values. The validation statistics (R^2v, SEP, RPDv) obtained by Xu et al. (2011) for black spruce and balsam fir were slightly higher for air-dried density (0.87, 25, 2.7), but lower for MOE (0.72, 1.0, 1.9) and MFA (0.56, 3.2, 0.9). A value of RPDv above 2.5 is usually defined as satisfactory for screening in a breeding program, whereas values of 5 to 10 are defined as adequate for quality control (Williams and Sobering 1993). However, based on the references cited in this article, the RPDv value is rarely above 3 for calibrations applied to solid wood. The calibrations obtained for BD, MOE, and MFA can thus be considered robust enough for operational use.

Figure 1 shows the correlations between SilviScan data (BD, MFA, MOE) and NIRS values obtained from the calibration and validation sets. Small deviations from linearity were observed for the highest values of BD (500 kg/m^3 and more). In this range, BD was underestimated by NIRS. For MFA, small deviations also occurred in extreme values (7° and less, 30° and more). In these ranges, MFA was also underestimated by NIRS. The same trends were observed with the prediction set. For MOE, no deviation was obvious. Several authors have also observed slight deviations from linearity at extreme values in density (Schimleck et al. 2001, Via 2010) and in MFA (Jones et al. 2005, So et al. 2013). The source of nonlinearity for these extreme values seems to be intrinsic to wood material given that the mathematical pretreatments were ineffective (Pérez-Marín et al. 2007). However, these deviations from linearity concern only a few samples in this study.

A large part of the variance in BD (85%), MFA (79%), and MOE (88%) was thus explained by FT-NIR spectra. The unexplained variance may be attributed to many sources. NIR light penetration is limited to a few millimeters from the surface as opposed to X-ray beam, which passes through the sample. NIRS may thus have not exactly captured the same properties as SilviScan. Furthermore, the transverse face was scanned by NIRS, whereas SilviScan scans samples on the radial face as previously discussed. Finally, in this study, MFA and MOE were estimated in 5-mm increments using Silviscan and in 7.5-mm increments using NIRS, which may have caused some approximations.

The autocorrelation between the trees from the same sites (site random effect) and between the spots from the same samples (sample random effect) was investigated. The classic PLS regression method proposed by The Unscrambler X software does not take into account the dependence between observations. The random effects were thus assessed on the residuals using mixed regressions (Proc MIXED, SAS 9.3). The random effect was highly significant for the sample and not significant for the site. However, the dependence between the measurements from a same sample is not surprising. This random effect was not considered in the development of calibrations that may have influenced the NIRS predictions at the spot scale and was certainly not considered for the MFA profile, which is the most important to determine the transition point.

A fixed effect related to the position of the measurement (spot) in the increment cores was also highly significant. The higher biases in BD and MOE were observed for spots collected close to the pith and bark. The extractive content is usually higher in these wood parts. Via et al. (2003) observed that MOE and MOR were poorly related to NIR spectra for pith wood in *Pinus palustris*, while density was strongly correlated. The authors explained that this lack of significance was perhaps attributable to the high concentration of resinous extractives near the pith. Furthermore, compression wood is also very frequent close to the pith. It could thus be interesting to consider the spot position as covariable in a PLS regression.

Two segment linear regressions

Table 3 shows the results of TSLR applied to the 127 MFA profiles obtained with SilviScan. The average transition age was 23 ± 7 years, varying between 8 and 43 years. The average MFA value at the transition point was 13.9° ± 3.2°. All the MFA profiles presented the same inverted J shape (Fig. 2). On average, the MFA value close to the pith was 32.3° ± 5.7°, whereas the MFA value close to the bark was 10.5° ± 2.1°. The average MFA value at the transition point was 2.3 times smaller than the MFA value close to the pith. Alteyrac et al. (2006) applied TSLR to ring area, maximum ring density, and ring MFA to determine the transition point of 36 black spruce trees harvested near Chibougamau, Québec. The transition age at 2.4 m was estimated at 14.0, 17.6, and 15.9 years, respectively. Yang and Hazenberg (1994) applied TSLR to tracheid length to determine the transition point of 10 black spruce trees harvested near Thunder Bay, Ontario. The transition varied between 11 and 21 years among the samples taken at breast height. The transition age estimated at 23 years in the present study is thus relatively similar to results presented in the literature.

Once the transition age became known, juvenile–mature wood properties were calculated. The proportion of mature wood was 82.5 ± 13.3 percent. There were highly significant differences in BD, MFA, and MOE between juvenile and mature wood using *t* tests for paired observations (Proc TTEST paired, SAS 9.3). Average values for mature wood were significantly higher than those for juvenile wood for BD (436.6 vs. 417.9 kg/m^3) and MOE (15.0 vs. 10.4 GPa), whereas for MFA, average value for mature wood was significantly lower than that for juvenile wood (12.6° vs. 20.2°). These results are consistent with the definition of juvenile and mature wood (Panshin and De Zeeuw 1980).

Table 4 shows the results of TSLR applied to the 127 MFA profiles obtained by NIRS. Average transition age was 21 ± 7 years, varying between 5 and 40 years. Average MFA value at the transition point was 15.4° ± 3.5°. All the MFA profiles presented the same inverted J shape (Fig. 2). The proportion of mature wood was 85.5 ± 11.3 percent. There were highly significant differences in BD, MFA, and MOE between juvenile and mature wood using *t* tests for paired observations (Proc TTEST paired, SAS 9.3). Average values for mature wood were significantly higher than those for juvenile wood for BD (435.4 vs. 426.4 kg/m^3) and MOE (14.6 vs. 10.5 GPa), whereas for MFA, average value for mature wood was significantly lower than that for juvenile wood (13.0° vs. 20.5°).

Of the 127 TSLR models, four and five models failed to converge using SilviScan data and NIRS data, respectively. Each of these cases was investigated. The presence of compression wood seems to be the main reason for nonconvergence when SilviScan data were used. Therefore, the data pretreatment applied to MFA profiles to remove the effect of compression wood was not sufficient

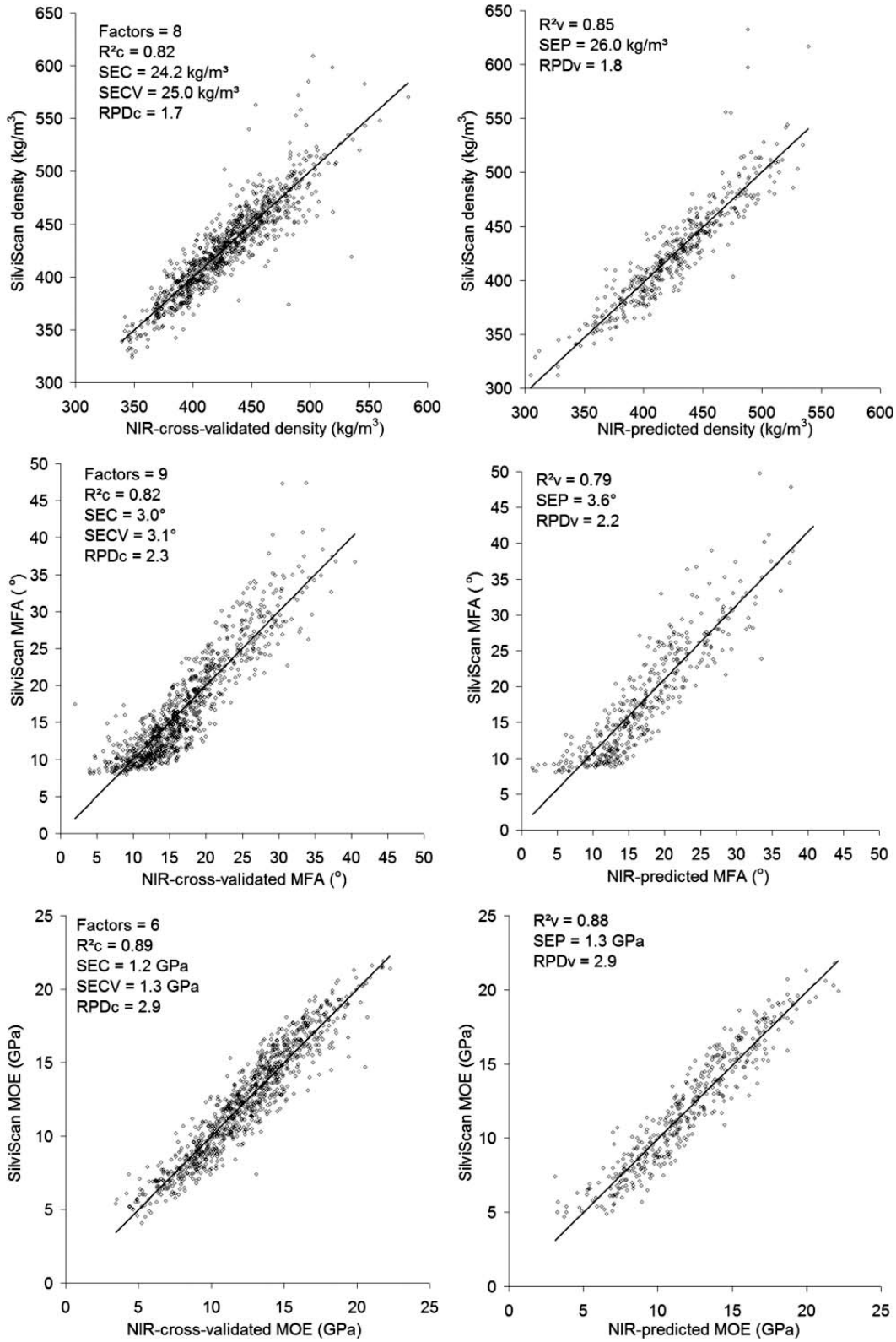

Figure 1.—(Left) Calibrations and (right) predictions for basic density (top panels), microfibril angle (MFA; middle panels), and modulus of elasticity (MOE; bottom panels).

for these samples. However the threshold filtering method has corrected 28 percent of the MFA values and helped the convergence of other models while increasing the measurement accuracy of the transition point (Fig. 3). Such pretreatment is thus strongly recommended for operational use. Moreover, it would be relevant to optimize this threshold filtering in function of transition age results rather than by trial and error. This pretreatment has also

*Table 3.—Statistics of juvenile and mature wood properties calculated from SilviScan data (*n = *127).*[a]

Wood property	Sample wood			Juvenile wood			Mature wood		
	Mean (SD)	Min.	Max.	Mean (SD)	Min.	Max.	Mean (SD)	Min.	Max.
Transition age (y)	22.8 (7.1)	8.0	43.0	—	—	—	—	—	—
Transition MFA (degrees)	13.9 (3.2)	9.3	25.3	—	—	—	—	—	—
Area proportion (%)	—	—	—	17.5 (13.3)	1.2	76.6	82.5 (13.3)	23.4	98.8
BD (kg/m^3)	431.8 (31.2)	361.7	509.1	417.9 (36.0)	333.6	538.2	436.6 (31.4)	367.5	516.8
MFA (degrees)	14.0 (3.1)	8.7	26.4	20.2 (3.7)	13.9	34.2	12.6 (3.2)	8.4	25.4
MOE (GPa)	14.1 (2.3)	8.7	19.0	10.4 (1.5)	6.2	13.7	15.0 (2.5)	8.9	20.3

[a] BD = basic density; MFA = microfibril angle; MOE = modulus of elasticity.

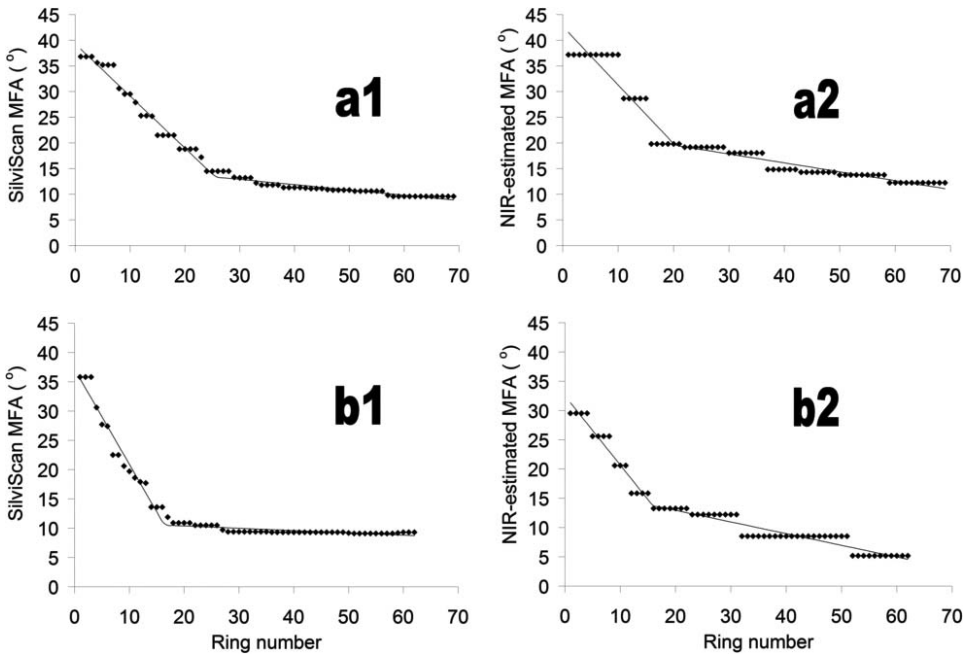

Figure 2.—Illustrations of segmented regressions fitted on microfibril angle (MFA) profiles obtained by (left) SilviScan and (right) near-infrared (NIR) spectroscopy for two samples (a and b).

made it possible to remove some unlikely NIRS predictions in the MFA profile. Nevertheless, a succession of prediction errors was the main reason for nonconvergence when NIRS data were used. A NIRS calibration is a predictive model. Even with an excellent calibration, errors due to variance (called *prediction errors*) and slight biases occur. However, after inspection, the transition ages of these nonconvergent models did not seem unlikely and the values were kept.

It should also be noted that TSLR was only applied in the present study to mature trees aged 45 years and older. Younger trees, which have less or no mature wood, could be sampled in an inventory. In this case, a standard linear regression should give a better fit than a TSLR, which could signal the absence of mature wood. Furthermore, MFA was estimated in 5-mm increments with SilviScan and in 7.5-mm increments with NIRS. The average ring width of the 127 samples was 0.95 mm. Consequently, such resolutions could not give a precision to the nearest ring. The

*Table 4.—Statistics of juvenile and mature wood properties calculated from NIRS data (*n = *127).*[a]

Wood property	Sample wood			Juvenile wood			Mature wood		
	Mean (SD)	Min.	Max.	Mean (SD)	Min.	Max.	Mean (SD)	Min.	Max.
Transition age (y)	20.6 (6.9)	5.0	40.0	—	—	—	—	—	—
Transition MFA (degrees)	15.4 (3.5)	6.2	23.2	—	—	—	—	—	—
Area proportion (%)	—	—	—	14.5 (11.3)	0.2	56.7	85.5 (11.3)	43.3	99.8
BD (kg/m^3)	432.6 (30.7)	355.8	511.2	426.4 (32.6)	352.2	549.3	435.4 (31.8)	355.4	515.3
MFA (degrees)	14.1 (3.2)	6.2	23.8	20.5 (3.3)	12.9	31.7	13.0 (3.5)	4.9	23.9
MOE (GPa)	14.0 (2.2)	8.9	19.1	10.5 (1.8)	6.3	14.1	14.6 (2.4)	8.9	20.0

[a] NIRS = near-infrared spectroscopy; BD = basic density; MFA = microfibril angle; MOE = modulus of elasticity.

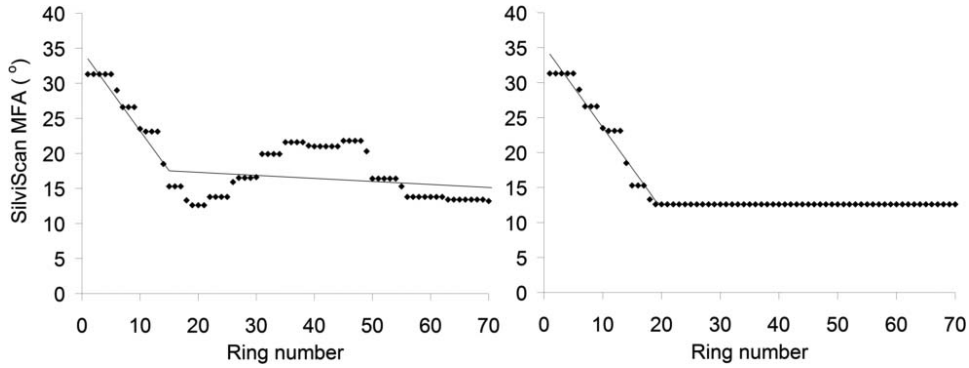

Figure 3.—Illustrations of segmented regressions fitted on (left) raw microfibril angle (MFA) profile obtained by SilviScan and (right) MFA profile corrected by the threshold filtering.

*Table 5.—Comparison between the SilviScan and NIRS estimates (*n = *127).*[a]

	Sample wood				Juvenile wood				Mature wood			
Wood property	*r*	Bias (SD)	Lower	Upper	*r*	Bias (SD)	Lower	Upper	*R*	Bias (SD)	Lower	Upper
Transition age (y)	0.59**	−2.2 (6.3)	−14.6	10.1	—	—	—	—	—	—	—	—
Transition MFA (degrees)	0.95**	−1.5 (1.1)	−3.7	0.7	—	—	—	—	—	—	—	—
Area proportion (%)	—	—	—	—	0.65**	−3.0 (10.4)	−23.4	17.5	0.65**	3.0 (10.4)	−17.5	23.4
BD (kg/m^3)	0.95**	0.9 (9.7)	−18.1	19.8	0.89**	8.4 (16.6)	−24.2	41.0	0.93**	−1.3 (11.5)	−23.8	21.3
MFA (degrees)	0.78**	0.1 (2.1)	−4.0	4.1	0.70**	0.3 (2.7)	−5.0	5.7	0.78**	0.4 (2.2)	−4.0	4.8
MOE (GPa)	0.91**	−0.2 (0.9)	−2.0	1.7	0.79**	0.1 (1.1)	−2.0	2.3	0.90**	−0.4 (1.1)	−2.6	1.8

[a] *r* = Pearson correlation coefficient; bias = mean prediction error, average of differences; lower = bias − 1.96 SD; upper = bias + 1.96 SD; asterisks = correlation is highly statistically significant ($P < 0.001$); BD = basic density; MFA = microfibril angle; MOE = modulus of elasticity.

determination of the transition age could also be more accurate with MFA determined or predicted at a resolution of 2 mm or less, particularly in the presence of very narrow growth rings.

Methods comparison for the determination of wood properties

The transition age and juvenile–mature wood properties obtained from SilviScan data (Table 3) were compared with values obtained from NIRS predicted data (Table 4). The two methods were compared using the correlation coefficient and the agreement. Table 5 shows that the correlations between the two data sets were moderate to high. The lowest correlations were observed for transition age ($r = 0.59$, $P < 0.001$) and juvenile–mature wood proportion ($r = 0.65$, $P < 0.001$). The lowest agreements were also observed for these properties. The transition age was slightly underestimated by NIRS with a mean prediction error (and 95% limits of agreement) of –2.2 ± 6.3 years (–14.6/10.1). The juvenile wood proportion was also slightly underestimated by NIRS with a mean prediction error (and 95% limits of agreement) of –3.0 ± 10.4 percent (–23.4/17.5). Excellent correlation ($r = 0.95$, $P < 0.001$) and agreement were obtained for transition MFA with −1.5° ± 1.1° (–3.7/0.7). Good to excellent correlations and agreements were also observed for juvenile–mature wood properties (Table 5).

The correlation and the agreement were thus notably higher for transition MFA than for transition age. Close to the transition point, MFA presents very few variations, as opposed to the transition age, which was strongly influenced by the measurement resolution (Fig. 2). For 86 of 127 (68%) samples, the transition age was similar (±5 y) to that obtained using SilviScan data. A few cases with greater discrepancies occurred despite the good calibration statistics for MFA. Discrepancies above 10 years for the transition age were observed for 12 of 127 (9%) samples, including extreme discrepancies above 15 years for three samples (2%). These cases were investigated, and the main observed cause also was the succession of prediction errors, which disturbed the MFA profile. For operational use, the performance of the NIRS calibration should not be inferior to that obtained for MFA in this study. In addition, some rules should be defined to detect potential outliers. Using the 0.05 and 0.95 percentiles of SilviScan measurements as thresholds, a transition MFA below 9° or above 21° could be considered as suspicious, as well as a transition age below 10 years or above 32 years. A better knowledge of the natural range of black spruce wood properties could help to define stronger rules. A larger sampling of all the natural ranges of growth conditions could thus be required.

Conclusions

NIRS potential to model MFA in order to automatically determine the transition from juvenile to mature wood was confirmed in this study. First, good to excellent calibrations (R^2v, RPDv) were obtained for BD (0.85, 1.8), MFA (0.79, 2.2), and MOE (0.88, 2.9). The TSLR method was then successfully applied to the MFA profile determined by SilviScan and to the MFA profile predicted by NIRS. However the NIRS transition age was poorly correlated to the SilviScan transition age ($r = 0.59$, $P < 0.001$). The ability of the method to precisely measure the transition age from a single sample should be improved to be ready for operational use. On the other hand, the suggested method was able to correctly estimate an average transition age for a

given population with a mean prediction error (and 95% limits of agreement) of –2.2 ± 6.3 years (–14.6/10.1).

The data pretreatment applied to MFA profiles improved the measurement accuracy of the transition point, and its use is strongly recommended for species with high proportions of compression wood. The difference in resolution between SilviScan data (every 5 mm) and NIRS predictions (every 7.5 mm) could partly explain the discrepancies observed in the estimation of transition age by NIRS. A better precision of the transition age could be obtained with MFA determined or predicted at a resolution of 2 mm or less, given the annual growth ring width in natural black spruce. Finally, a better knowledge of the natural range for MFA in black spruce could help to identify unlikely values.

NIRS appears to be a suitable and economic alternative to SilviScan to assess the transition age, even if the method accuracy must still be improved for operational use. Such a method could be integrated into a NIRS system for rapid determination of the transition age and juvenile–mature wood properties of an increment core. Thousands of samples from trees grown in various conditions could be assessed. Large-scale research could thus help to obtain a better understanding of the factors that influence the transition. In addition, this method could be adapted to any species with a MFA profile in an inverted J shape.

Acknowledgments

This research was funded by the Fonds de recherche du Québec–Nature et technologies and the Ministère des Ressources naturelles du Québec. The samples were provided by the Canadian Wood Fibre Centre, Canadian Forest Service, Natural Resources Canada. The authors thank the Centre de recherche sur le bois de l'Université Laval for material support and are especially grateful to Professor Tatjana Stevanovic for the use of NIR spectrometer. Thanks also to the FPInnovations team for providing the fiber database. Thanks to Sébastien Cortade for help with sample preparation and spectra collection. Thanks to Martin Riopel for statistical support.

Literature Cited

Alteyrac, J., A. Cloutier, and S. Y. Zhang. 2006. Characterization of juvenile wood to mature wood transition age in black spruce (*Picea mariana* (Mill.) B.S.P.) at different stand densities and sampling heights. *Wood Sci. Technol*. 40(2):124–138.

Barnett, J. R. and V. A. Bonham. 2004. Cellulose microfibril angle in the cell wall of wood fibres. *Biol. Rev*. 79(2):461–472.

Bhat, K. M., P. B. Priya, and P. Rugmini. 2001. Characterisation of juvenile wood in teak. *Wood Sci. Technol*. 34(6):517–532.

Bland, J. M. and D. G. Altman. 1995. Comparing methods of measurement: Why plotting difference against standard method is misleading. *Lancet* 346(8982):1085–1087.

Briggs, D. 2010. Enhancing forest value productivity through fiber quality. *J. Forestry* 108(4):174–182.

Cieszewski, C. J., M. Strub, F. Antony, P. Bettinger, J. Dahlen, and R. C. Lowe. 2013. Wood quality assessment of tree trunk from the tree branch sample and auxiliary data based on NIR spectroscopy and SilviScan. *Math. Comput. Forestry Nat.-Res. Sci*. 5(26):86–111.

Clark, A., III, R. F. Daniels, and L. Jordan. 2006. Juvenile/mature wood transition in loblolly pine as defined by annual ring specific gravity, proportion of latewood, and microfibril angle. *Wood Fiber Sci*. 38(2):292–299.

Donaldson, L. 2008. Microfibril angle: Measurement, variation and relationships—A review. *IAWA J*. 29(4):345–386.

Evans, R. 1999. A variance approach to the X-ray diffractometric estimation of microfibril angle in wood. *Appita J*. 52(4):283–289.

Evans, R., S. Stringer, and R. Kibblewhite. 2000. Variation of microfibril angle, density and fibre orientation in twenty-nine *Eucalyptus nitens* trees. *Appita J*. 53(6):450–457.

Hein, P., B. Clair, L. Brancheriau, and G. Chaix. 2010. Predicting microfibril angle in *Eucalyptus* wood from different wood faces and surface qualities using near infrared spectra. *J. Near Infrared Spectrosc*. 18(6):455–464.

Jessome, A. P. 1995. Strength and related properties of woods grown in Canada. SP-514F. Forintek Canada Corp., Ottawa, Ontario. 37 pp.

Jones, P. D., L. R. Schimleck, G. F. Peter, R. F. Daniels, and A. Clark III. 2005. Nondestructive estimation of *Pinus taeda* L. wood properties for samples from a wide range of sites in Georgia. *Can. J. Forest Res*. 35(1):85–92.

Jozsa, L. A. and G. R. Middleton. 1994. A discussion of wood quality attributes and their practical implications. SP-34. Forintek Canada Corp., Vancouver, British Columbia. 42 pp.

Lessard, E. 2013. Modeling and mapping wood fiber attributes using environmental and forest inventory data: Case of Newfoundland's boreal forest. Master's thesis in geographic sciences. Université de Sherbrooke, Québec, Canada. 103 pp. (In French.)

Lessard, E., R. A. Fournier, J. E. Luther, M. J. Mazerolle, and O. R. Van Lier. 2014. Modeling wood fiber attributes using forest inventory and environmental data for Newfoundland's boreal forest. *Forest Ecol. Manag*. 313:307–318.

Meder, R., T. Trung, and L. Schimleck. 2010. Guest editorial: Seeing the wood in the trees: Unleashing the secrets of wood via near infrared spectroscopy. *J. Near Infrared Spectrosc*. 18(6):v–vii.

Panshin, A. J. and C. De Zeeuw. 1980. Textbook of Wood Technology: Structure, Identification, Properties, and Uses of the Commercial Woods of the United States and Canada. 4th ed. McGraw-Hill, New York. 722 pp.

Pérez-Marín, D., A. Garrido-Varo, and J. E. Guerrero. 2007. Non-linear regression methods in NIRS quantitative analysis. *Talanta* 72(1):28–42.

Ryan, S. E. and L. S. Porth. 2007. A tutorial on the piecewise regression approach applied to bedload transport data. General Technical Report RMRS-GTR-189. USDA Forest Service, Rocky Mountain Research Station, Fort Collins, Colorado. 41 pp.

Schimleck, L. R. and R. Evans. 2002. Estimation of microfibril angle of increment cores by near infrared spectroscopy. *IAWA J*. 23(3):225–234.

Schimleck, L. R., R. Evans, and J. Ilic. 2001. Estimation of *Eucalyptus delegatensis* wood properties by near infrared spectroscopy. *Can. J. Forest Res*. 31(10):1671–1675.

Schimleck, L. R., P. D. Jones, A. Clark III, R. F. Daniels, and G. F. Peter. 2005a. Near infrared spectroscopy for the nondestructive estimation of clear wood properties of *Pinus taeda* L. from the southern United States. *Forest Prod. J*. 55(12):21–28.

Schimleck, L. R., R. Stürzenbecher, C. Mora, P. D. Jones, and R. F. Daniels. 2005b. Comparison of *Pinus taeda* L. wood property calibrations based on NIR spectra from the radial-longitudinal and radial-transverse faces of wooden strips. *Holzforschung* 59(2):214–218.

Siau, J. F. 1995. Wood: Influence of moisture on physical properties. Department of Wood Science and Forest Products, Virginia Polytechnic Institute and State University, Blacksburg. 227 pp.

Siesler, H. W., Y. Ozaki, S. Kawata, and H. M. Heise. 2002. Near-Infrared Spectroscopy: Principles, Instruments, Applications. Wiley-VCH, Weinheim, Germany. 348 pp.

So, C.-L., J. H. Myszewski, T. Elder, and L. H. Groom. 2013. Rapid analysis of the microfibril angle of loblolly pine from two test sites using near-infrared analysis. *Forestry Chron*. 89(5):639–645.

Tsuchikawa, S. 2007. A review of recent near infrared research for wood and paper. *Appl. Spectrosc. Rev*. 42(1):43–71.

Via, B. 2010. Prediction of oriented strand board wood strand density by near infrared and Fourier transform infrared reflectance spectroscopy. *J. Near Infrared Spectrosc*. 18(6):491–498.

Via, B. K., T. F. Shupe, L. H. Groom, M. Stine, and C.-L. So. 2003. Multivariate modelling of density, strength and stiffness from near infrared spectra for mature, juvenile and pith wood of longleaf pine (*Pinus palustris*). *J. Near Infrared Spectrosc*. 11(5):365–378.

Via, B. K., C. L. So, T. F. Shupe, L. H. Groom, and J. Wikaira. 2009. Mechanical response of longleaf pine to variation in microfibril angle,

chemistry associated wavelengths, density, and radial position. *Compos. Part A* 40(1):60–66.

Viereck, L. A. and W. F. Johnston. 1990. *Picea mariana* (Mill.) B.S.P.—Black spruce. *In:* Silvics of North America. Vol. 1. Conifers. Agricultural Handbook 654. R. M. Burns and B. H. Honkala (Eds.). USDA Forest Service, Washington, D.C. pp. 227–237.

Wang, M. and J. D. Stewart. 2012. Determining the transition from juvenile to mature wood microfibril angle in lodgepole pine: A comparison of six different two-segment models. *Ann. Forest Sci*. 69(8):927–937.

Williams, P. C. and D. C. Sobering. 1993. Comparison of commercial near infrared transmittance and reflectance instruments for analysis of whole grains and seeds. *J. Near Infrared Spectrosc*. 1(1):25–32.

Xu, Q., M. Qin, Y. Ni, M. Defo, B. Dalpke, and G. Sherson. 2011. Predictions of wood density and module of elasticity of balsam fir (*Abies balsamea*) and black spruce (*Picea mariana*) from near infrared spectral analyses. *Can. J. Forest Res*. 41(2):352–358.

Yang, K. C. and G. Hazenberg. 1994. Impact of spacing on tracheid length, relative density, and growth rate of juvenile wood and mature wood in *Picea mariana*. *Can. J. Forest Res*. 24(5):996–1007.